To be presented at XVth International
Conference on High Energy Physics,
Kiev, USSR, August 26-Sept. 4, 1970

UCRL-20079
Preprint

Conf-700806--45

MASTER

A MEASUREMENT OF THE BRANCHING RATIO $K^+ \to e^+\nu/K^+ \to \mu^+\nu$

A. R. Clark, B. Cork, T. Elioff, L. T. Kerth,
J. F. McReynolds, D. Newton, and W. A. Wenzel

August 1970

AEC Contract No. W-7405-eng-48

LAWRENCE RADIATION LABORATORY
UNIVERSITY of CALIFORNIA BERKELEY

UCRL-20079

DISCLAIMER

To be presented at XVth International Conference on High Energy Physics, Kiev, USSR, August 26–Sept. 4, 1970

UCRL–20079

A MEASUREMENT OF THE BRANCHING RATIO $K^+ \to e^+\nu/K^+ \to \mu^+\nu$ *

A. R. Clark, B. Cork,** T. Elioff, L. T. Kerth, J. F. McReynolds, D. Newton,*** and W. A. Wenzel

Lawrence Radiation Laboratory
University of California
Berkeley, California

August 20, 1970

The rate for Ke2 decays ($K^+ \to e^+\nu$) is a severe test of the V–A theory of weak interactions. The K meson can couple to the vacuum (leptons) either as a pseudoscaler (P) or axial vector (A). The ratio of the Ke2 rate to the Kμ2 rate is:

$$R_{TH} = \frac{\Gamma\,(K \to e\nu)}{\Gamma\,(K \to \mu\nu)} = \frac{(m_k^{\,2} - m_e^{\,2})}{(m_k^{\,2} - m_\mu^{\,2})} \left(\frac{f_A\, m_e/m_k + f_p}{f_A\, m_\mu/m_k + f_p}\right)^2 C_\gamma \ ,$$

where C_γ is an experiment–dependent electromagnetic correction;[1] in this experiment $C_\gamma = 0.861$. For pure A and pure P we have:

$$R_{TH}(\text{pure A}) = C_\gamma\,[(m_k^{\,2} - m_e^{\,2})/(m_k^{\,2} - m_\mu^{\,2})]\,(m_e^{\,2}/\,m_\mu^{\,2}) = 2.185 \times 10^{-5}$$

$$R_{TH}(\text{pure P}) = C_\gamma\,(m_k^{\,2} - m_e^{\,2})/(m_k^{\,2} - m_\mu^{\,2}) = .901.$$

For pion decay, the experimental results[2] give

$$\frac{R_{exp}}{R_{TH}(\text{pure A})} = 1.00 \pm 0.03$$

Two other groups have performed this experiment, Mann et al.[3] at the Princeton-Penn accelerator with 7 ± 4 events and Jones et al.[4] at Oxford with $10^{+3.7}_{-2.6}$.

The experimental setup at the Bevatron is shown in Figure 1. A double focused electrostatically-separated K^+ beam of momentum 540 MeV/c ± 2% was stopped in a polyethylene target. The π:K ratio was 50:1 after separation. The kaon beam passed through a 3 mm scintillator (S1) and a 5 mm Lucite threshold Cerenkov counter (C_π) located at the mass slit. The Cerenkov counter was used to veto pions in the beam. The beam entered the spectrometer magnet on the axis, passed through a 6 mm scintillator (S2), a 27 cm Be degrader, a 3 mm scintillator (S3), a 4-gap spark chamber, and stopped in a 70 mm long x 31 mm diam. polyethylene stopper located 12 cm downstream of the median plane of the magnet. The stopper was covered on the side and downstream surfaces by a 3 mm thick sleeve scintillator. Beam pions were rejected by time of flight (S1-S2), a count from C_π, a pulse less than 2 x minimum in S3, or a prompt count from S4.

Decay secondaries were allowed one orbit in the M5 spectrometer. The magnetic field was shaped so that particles leaving the stopper with polar angles in the range 70°-115° were focused back to a point on the magnet axis 12 cm upstream of the median plane. The field in the center of the magnet for Ke2 runs was 18,600 gauss, decreasing to 15,700 gauss at the maximum orbit radius of 90 cm. The design of the trigger system was based on the fact that, of the charged particles from all K-decay modes, the electrons from Ke2 decays have the highest momenta, and hence will reach the largest radii in the magnet. Secondaries in a momentum bite of $\Delta P/P = .10$ were required to pass through at least one 6 mm x 80 cm x 13 cm scimitar-shaped counter at an average spherical radius of 80 cm from the magnet center. These counters were shaped to give a sharp lower momentum cutoff to exclude triggers from $K\rightarrow e\nu\pi^0$ decays. There were nine such outer radius counters, (O) each in timed coincidence with the corresponding members of an 18-scintillator hodoscope (I) of 3 mm x 8 cm x 50 cm counters at 20 cm radius. Orbits in the proper momentum and angular bite starting at the stopper passed through S4 and at least 10 cm of a 300 psi ethane gas Cherenkov counter (E), an I counter, and a cylindrical four-gap spark chamber at 24 cm radius. With each O counter was a set of two two-gap foam plate spark chambers. Returning to the axis of the magnet, the orbiting particle passed again through the cylindrical spark chamber and an I-hodoscope counter approximately 180° from the outgoing track, and into a 38 mm thick lead sleeve of 18 cm outside radius, in which electrons were preferentially absorbed. Inside the lead sleeve was a smaller cylindrical spark chamber in which surviving muons were identified. Within this chamber was a 6 mm cylindrical scintillator (M) to further identify muons.

The ethane Cherenkov counter efficiency was calibrated in a test beam and then checked during the run using Ke3-decay electrons at 145-160 MeV/c; both procedures gave an efficiency of 0.98 for detecting electrons.

The spark chambers were triggered on a stopping K (S1–S2–S3–$\overline{C}_{\pi}$–$\overline{S}$4), with a delayed decay and orbit (S4–I_i–O_j–I_k) signature and an electron signal (E). An M pulse in coincidence with the orbit signature lit a light which was photographed with the spark chambers.

Chambers on the inner radius (out to 26 cm) were viewed directly through a hole in the magnet poletip. Outer-radius chambers were seen through a fish-eye optical system, with a maximum demagnification of 300:1. All events were scanned and measured with a computer-controlled precision CRT scanning system (SASS); spatial and momentum reconstruction were done on a CDC-6600 computer. Each event was required to have the secondary orbit originate in the stopper and to have $\chi^2 \leq 3.5$ per degree of freedom for the orbit fit.

Analysis of 60% of the data yielded 45,000 candidates for Ke2 decays; the secondary momentum spectra for these candidates is shown in Figures 2a and 2b for events with and without a signal from the M scintillator, respectively. Most of these candidates are background from Kμ2 decays with a delta ray or an accidental count in E. To effect the background subtraction, events with secondary momentum P > 235 MeV/c were rescanned and classified as either electron candidates (Figures 3b, 4b) or muon events (Figures 3a, 4a), according to the appearance of the track in the cylindrical chamber within the lead cylinder. Muons were identified with 95% accuracy, while 1% of the electrons were identified as muons. The shape of this muon spectrum was used for the background subtraction after normalization to the electron-candidate spectrum in the 235, 236, 237, 238, and 239 MeV/c bins. The Ke2 spectrum after background subtraction is shown in Figures 3c, 4c and 5.

Normalization runs for the Kμ2 rate were made with the magnet set to capture Kμ2 events, without the electron requirement. Overall normalization was made to the number of K decays ($S1-S2-S3-\overline{C}_{\pi}-\overline{S4}$) in each run. The Kμ2 secondary momentum spectrum is shown in Figure 2c.

The Kμ2 distributions have a measured center of 233.7 MeV/c, 1.9 MeV/c low, due to a magnet calibration error. The center of the electron distribution excluding bremstrahlung was therefore taken to be 245.0 MeV/c.

Outer bremstrahlung required a significant correction to the observed rate because the electrons passed through an average of .0930 radiation lengths before the midpoint of the orbit; only 0.638 of the electrons lost less than 5 MeV/c due to these effects.[5] Corrections for virtual photons and inner bremstrahlung give an additional factor of 0.861[1].

From 60% of the data so far analyzed, 66 ± 11 electron events with momentum greater than 240 MeV/c have been found in 72.3×10^6 stopping K decays.

In calibration runs, 6270 muons with momenta from 229 to 239 MeV/c have been found in 89,956 K decays. These numbers lead to a relative branching ratio of $2.15 \pm .35 \times 10^{-5}$. Assuming that $|f_p| \leq |\frac{m_e}{m_k} f_A|$, with f_p and f_A relatively real, this branching ratio implies

$$R_{exp} = 2.15 \pm .35 \times 10^{-5} \simeq 1.048 \left(\frac{m_e}{m_\mu}\right)^2 \left[1 + 2 \frac{m_k}{m_e} \frac{f_p}{f_A} \left(1 - \frac{m_e}{m_\mu}\right)\right] C_\gamma$$

or

$$\frac{f_p}{\frac{m_e}{m_k} f_A} = .502 \left[\frac{R_{exp}}{R(\text{pure A})} - 1\right] \simeq -.008 \pm .076$$

REFERENCES

1. Toichiro Kinoshita, Phys. Rev. Letters 2, 477 (1959).

2. S. Gasiorowicz, Elementary Particle Physics, Wiley, New York (1966), pp 504–507.

3. D. R. Bowen, A. K. Mann, W. K. McFarlane, A. D. Franklin, E. B. Hughes, R. L. Imlay, G. K. O'Neill, and D. H. Reading, Phys. Rev. 154, 1314 (1967).

4. D. R. Botterill, R. M. Brown, I. F. Corbett, G. Culligan, J. M. Emmerson, R. C. Field, J. Garvey, P. B. Jones, N. Middlemas, D. Newton, T. W. Quirk, G. L. Salmon, P. Steinberg, and W. S. C. Williams, Phys. Rev. 171, 1402 (1968).

5. W. Heitler, The Quantum Theory of Radiation, Clarendon Press, Oxford (1954), pp 368–382.

* This work was done under the auspices of the U. S. Atomic Energy Commission.

** Present address: Argonne National Laboratory, Illinois.

*** Present address: University of Lancaster, England.

FIGURE CAPTIONS

Figure 1 (a) Spectrometer side view.

(b) Axial view of spectrometer; section taken through median plane of the magnet. A typical muon orbit is shown.

Figure 2 Secondary momentum spectra:

(a) Data taken with Ke2 trigger accompanied by a signal from the M scintillator.

(b) Data taken with Ke2 trigger, not accompanied by a signal from the M scintillator.

(c) Data taken with Kμ2 trigger (M required), for normalization.

Figure 3 Data from Figure 2a (Ke2 trigger, accompanied by M signal), after visual classification into muon and electron categories:

(a) Muon events.

(b) Electron candidates.

(c) Electron events after background subtraction (see text).

Figure 4 Data from Figure 2b (Ke2 trigger, not accompanied by M signal), after visual classification into muon and electron categories:

(a) Muon events.

(b) Electron candidates.

(c) Electron events after background subtraction (see text).

Figure 5 Final electron spectrum (sum of data from Figures 3c and 4c). The curve is to guide the eye; it has not been fitted.

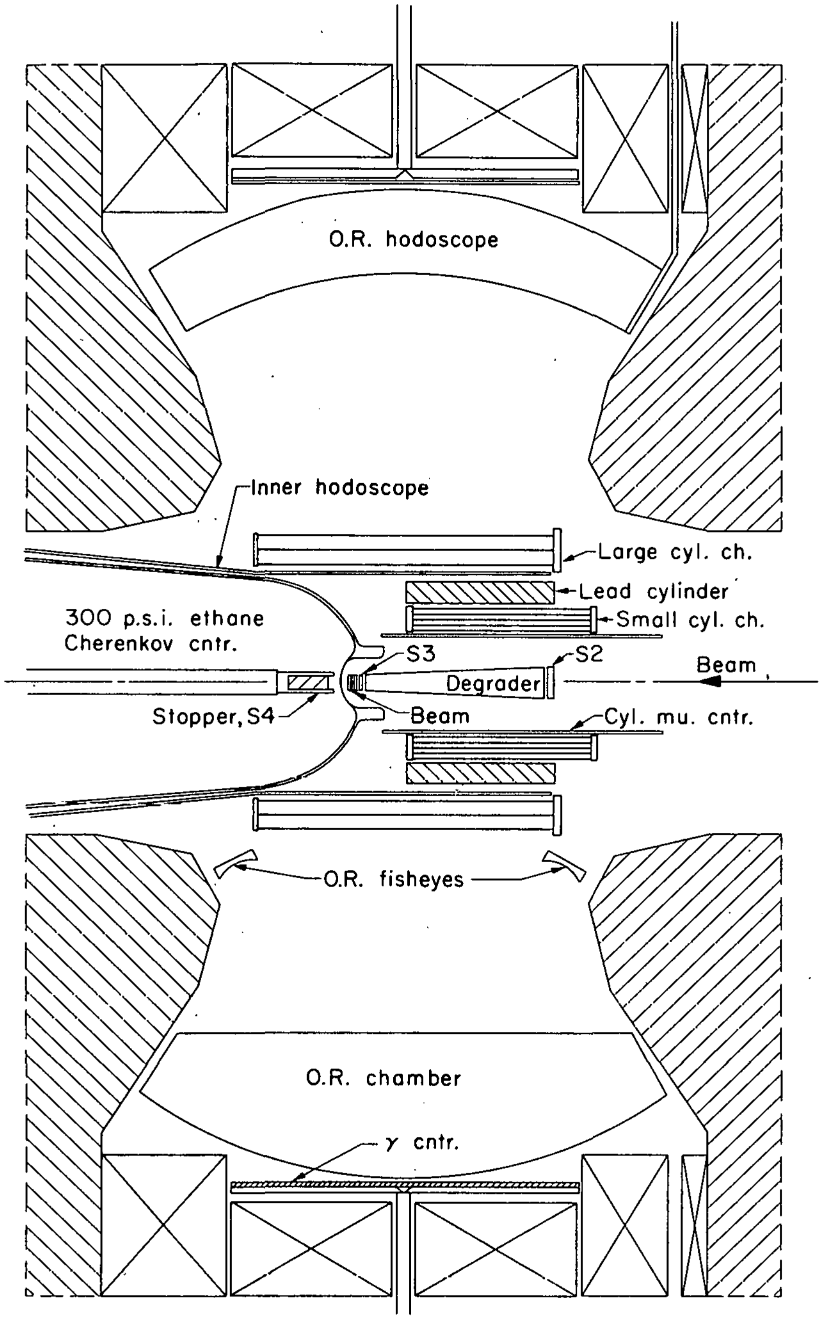

Ke2 magnet interior
(O.R.=outer radius)

XBL 708-3552

Figure 1a

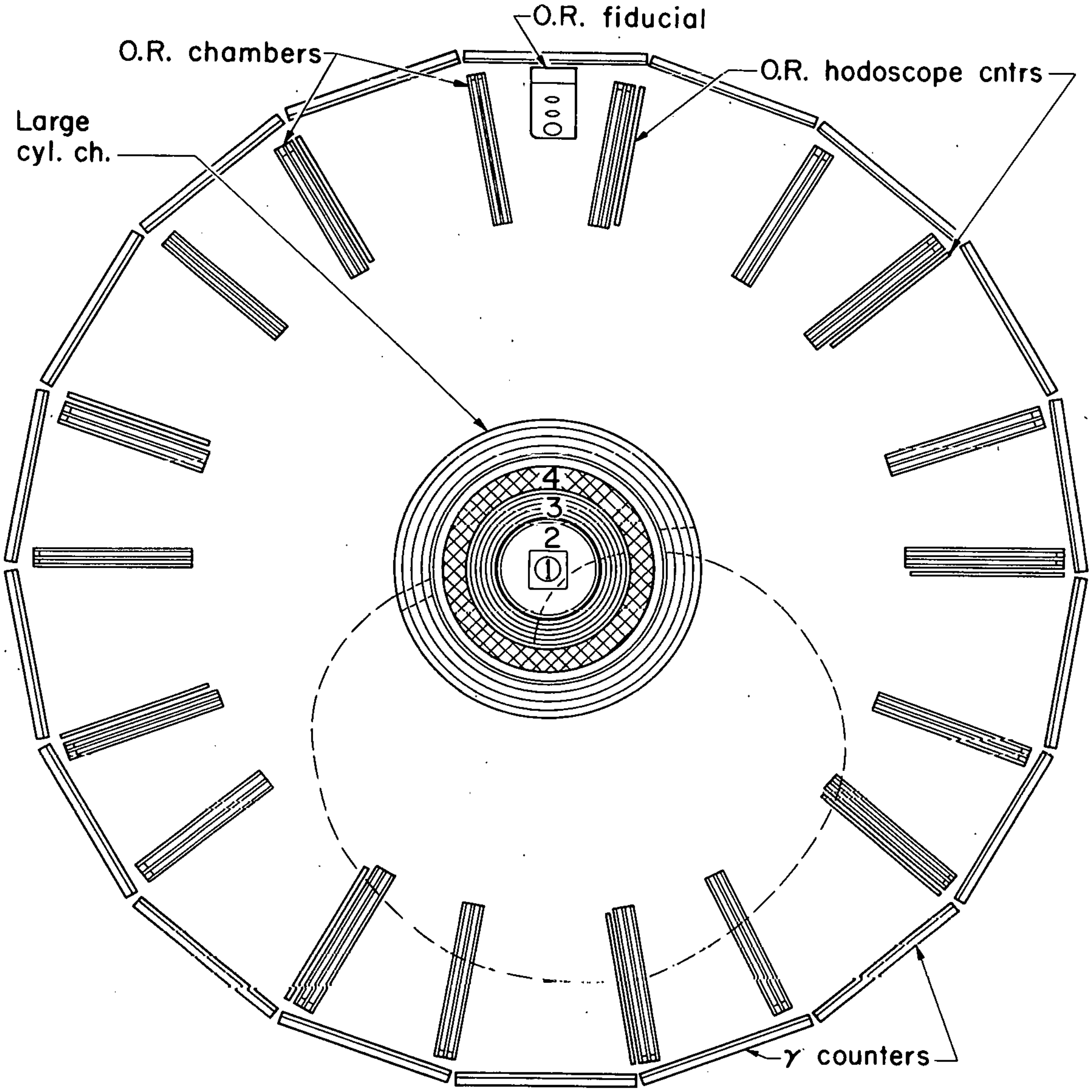

Ke2 magnet interior with typical orbit

1 Degrader
2 Cylindrical μ counter
3 Small cylindrical chamber
4 Lead cylinder

XBL708-3553

Figure 1b

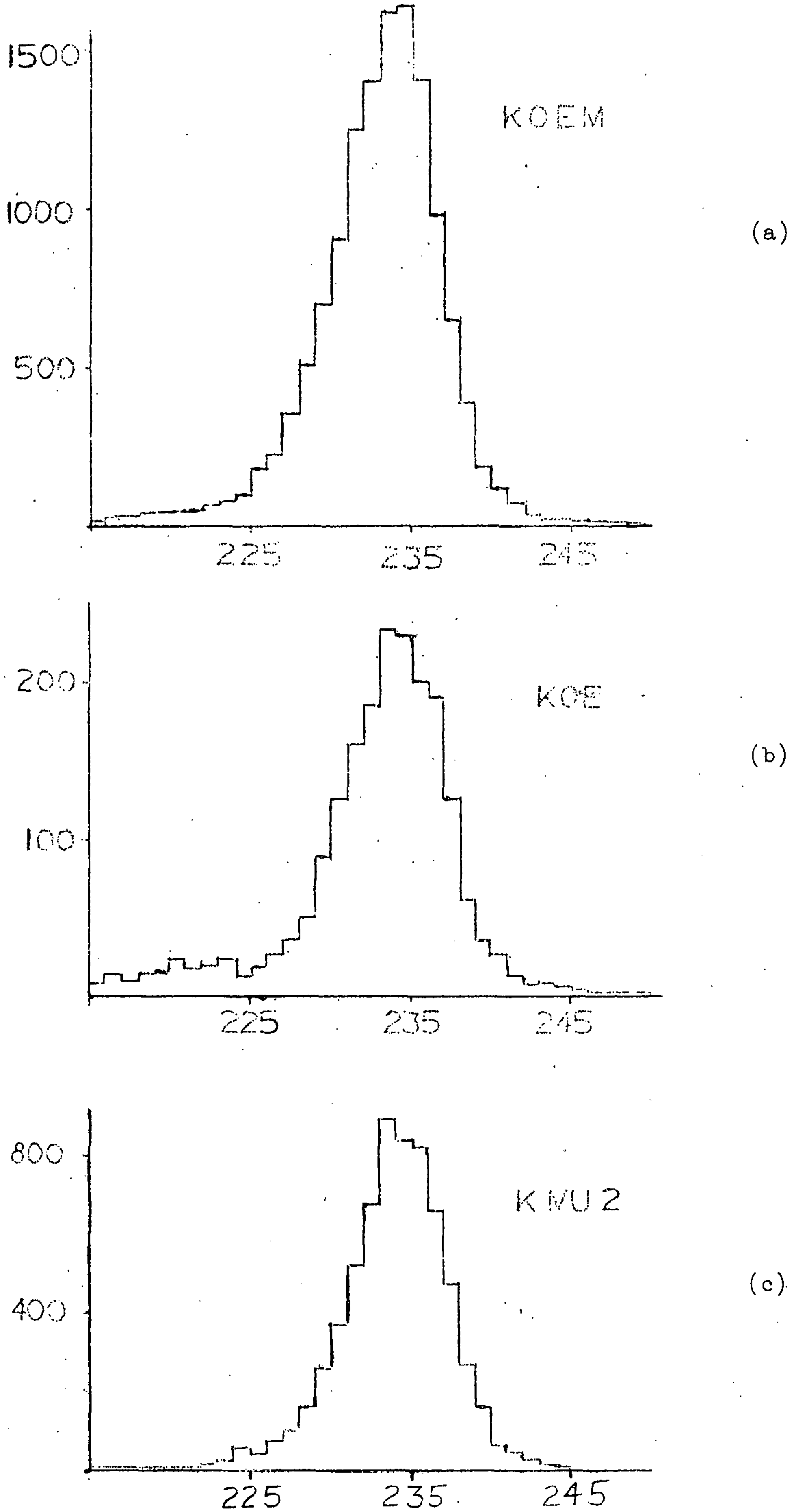
1500
1000
500
KOEM
225
235
245
(a)
200
100
KOE
225
235
245
(b)
800
400
K MU 2
225
235
245
(c)

Figure 2

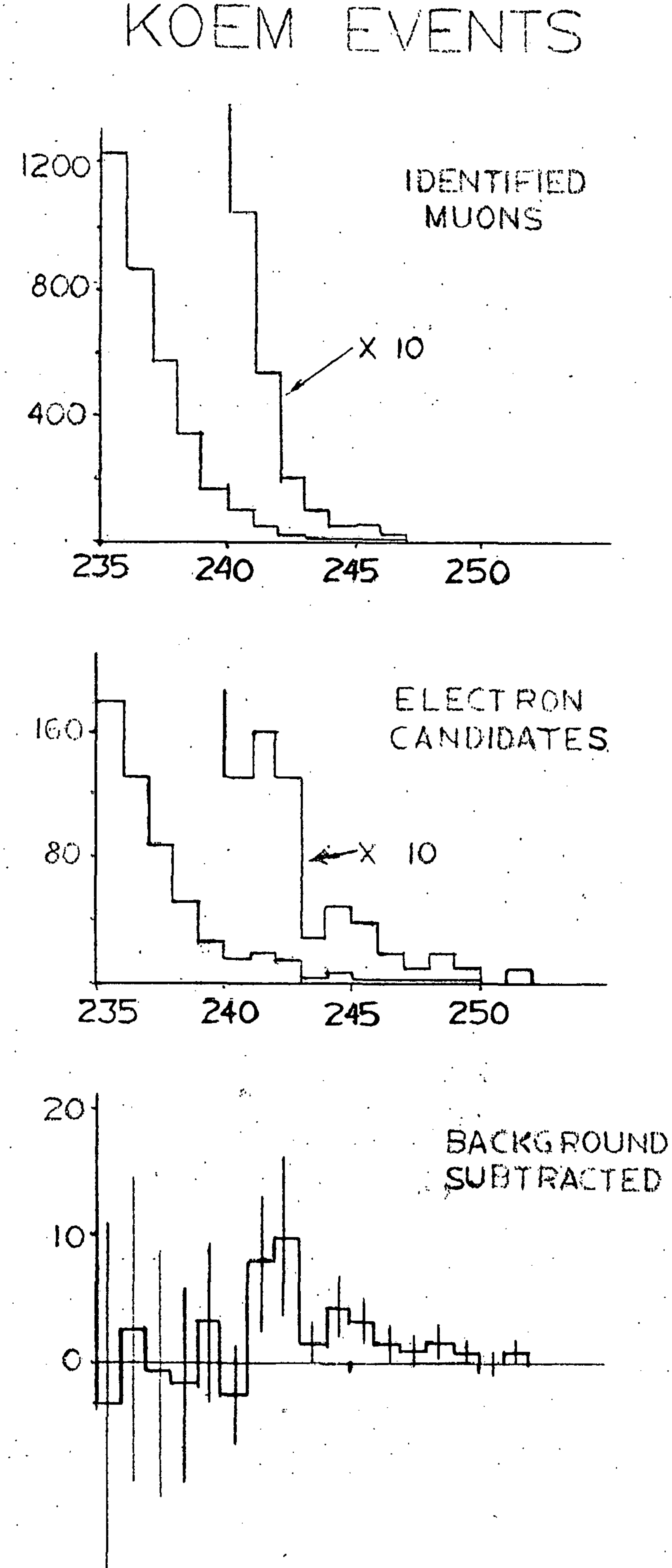
KOEM EVENTS
1200
800
400
IDENTIFIED MUONS
X 10
235
240
245
250
160
80
ELECTRON CANDIDATES
X 10
235
240
245
250
20
10
0
BACKGROUND SUBTRACTED

(a)

(b)

(c)

Figure 3

KOE EVENTS

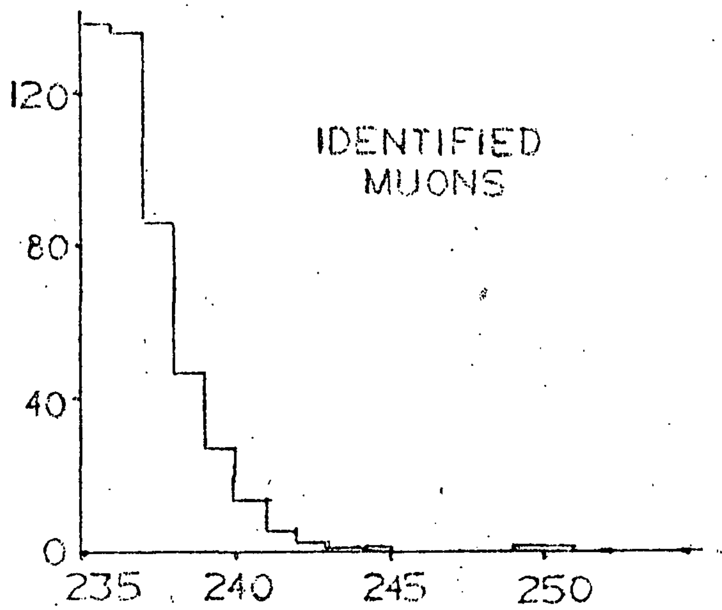

(a)

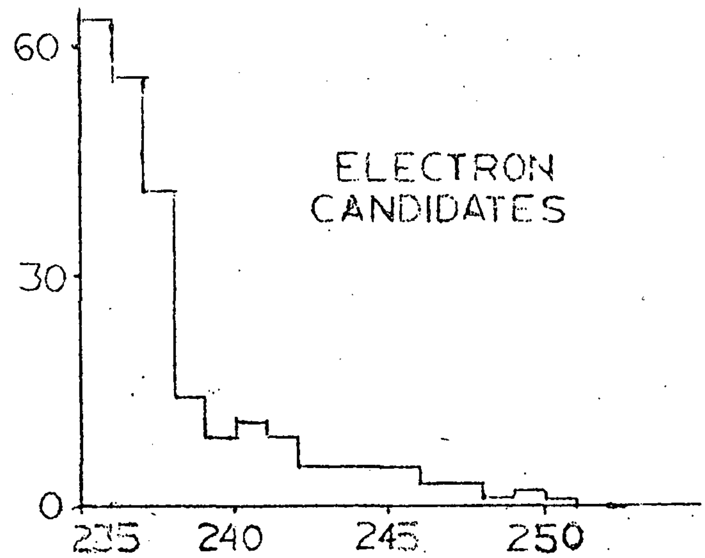

(b)

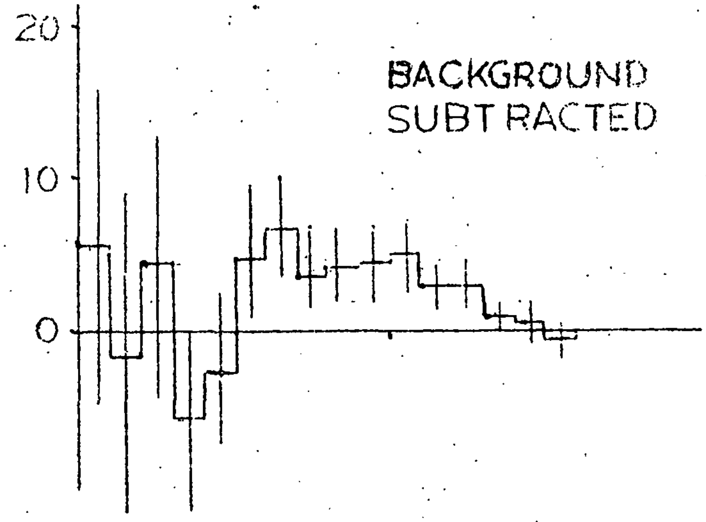

(c)

Figure 4

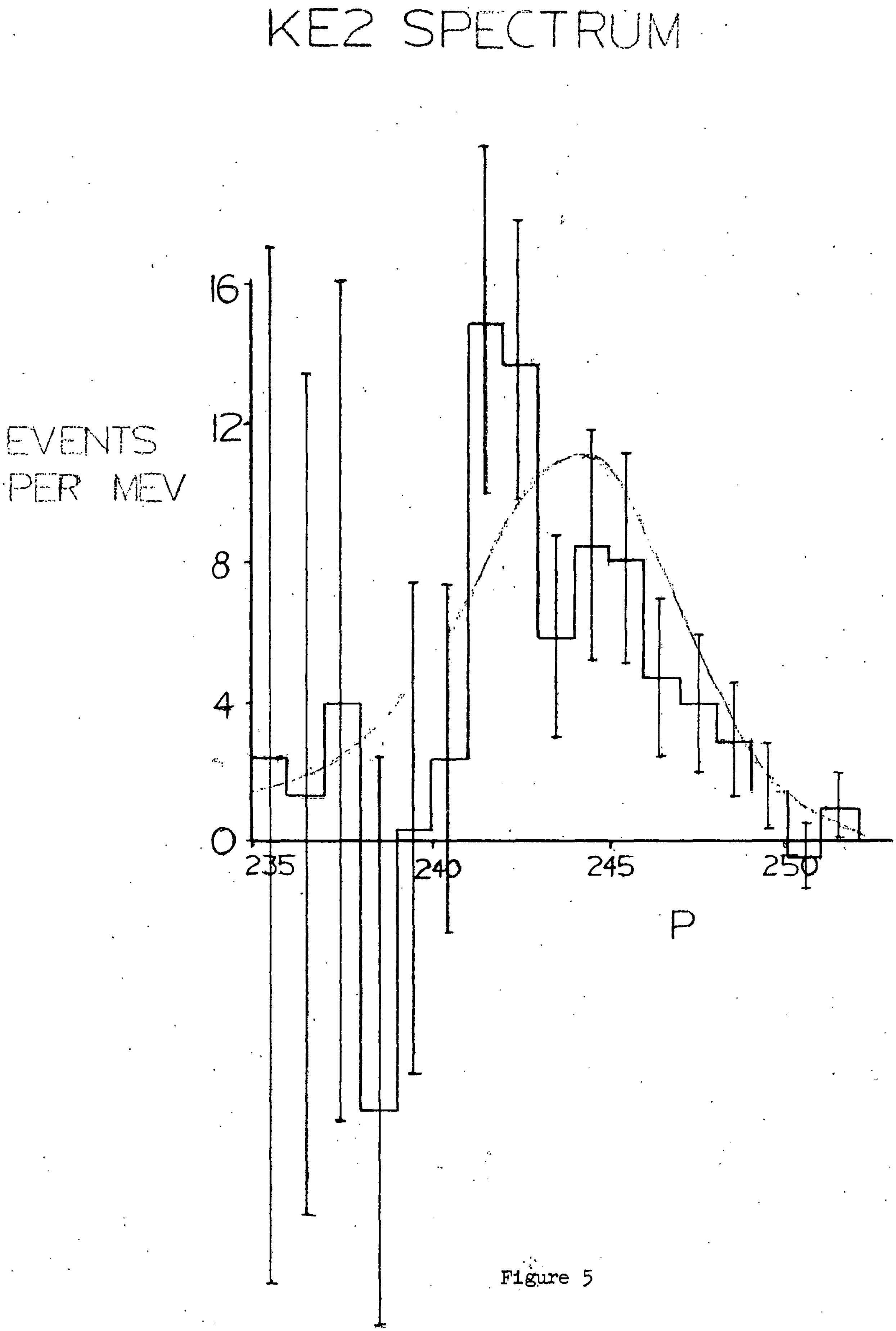

Figure 5

TECHNICAL INFORMATION DIVISION
LAWRENCE RADIATION LABORATORY
UNIVERSITY OF CALIFORNIA
BERKELEY, CALIFORNIA 94720